Supplementary Information

Highly efficient Zn: $CuInSe_2$/ZnS quantum dots for near-infrared optical wireless communications

Lizhao Nie,[a,b] Linqi Chen,*[b] Jingzhou Li,*[c] Yijing Wang,[c] Xiaoxia Wang,*[a] Long Zhang,[b,c] Hongxing Dong[b,c] and Anlian Pan*[a,d]

[a] College of Materials Science and Engineering, Hunan University, Changsha 410082, China.

[b] Key Laboratory of Materials for High-Power Laser, Shanghai Institute of Optics and Fine Mechanics, Chinese Academy of Sciences, Shanghai 201800, China.

[c] Hangzhou Institute for Advanced Study, University of Chinese Academy of Sciences, No.1, Sub-Lane Xiangshan, Xihu District, Hangzhou 310024, China.

[d] School of Physics and Electronics, Hunan Normal University, Changsha 410081, China.

* Corresponding author: chenlq@siom.ac.cn; lijingzhou@ucas.ac.cn; wangxiaoxia@hnu.edu.cn; Anlian.Pan@hnu.edu.cn

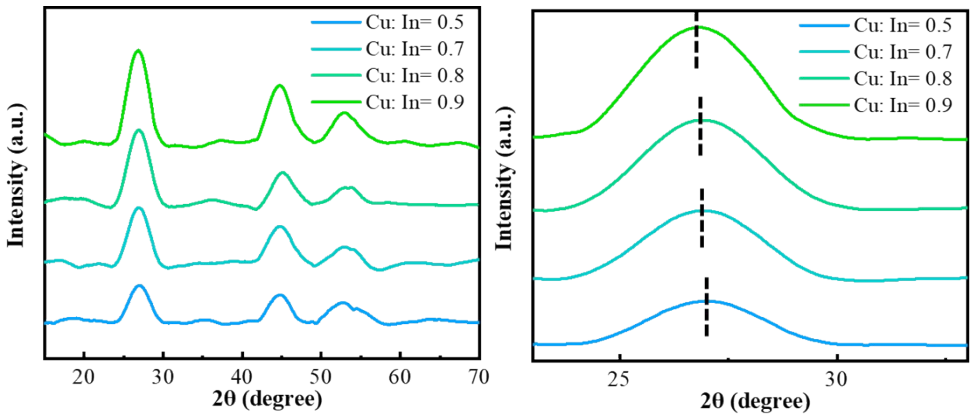

Fig. S1 Characteristic peak diffraction angles in XRD spectra shift to smaller angles with increasing copper ratio.

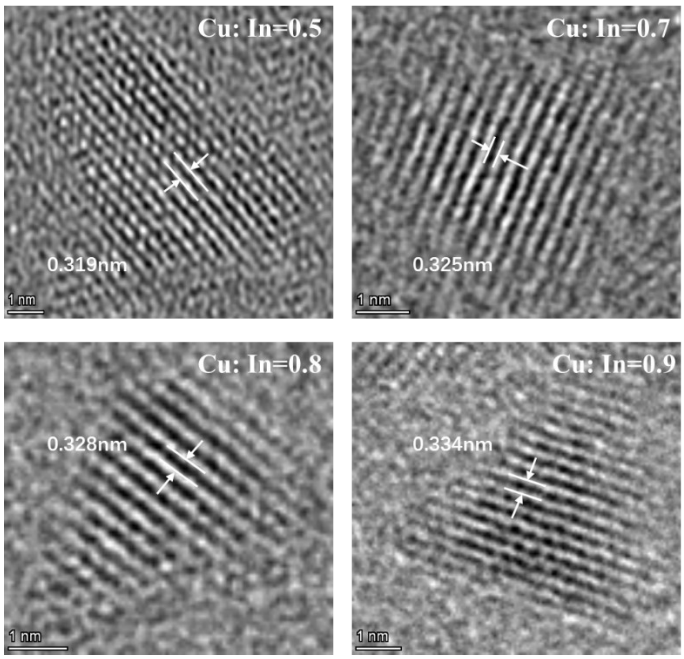

Fig. S2 Interplanar spacing of quantum dots gradually increases with increasing copper ratio.

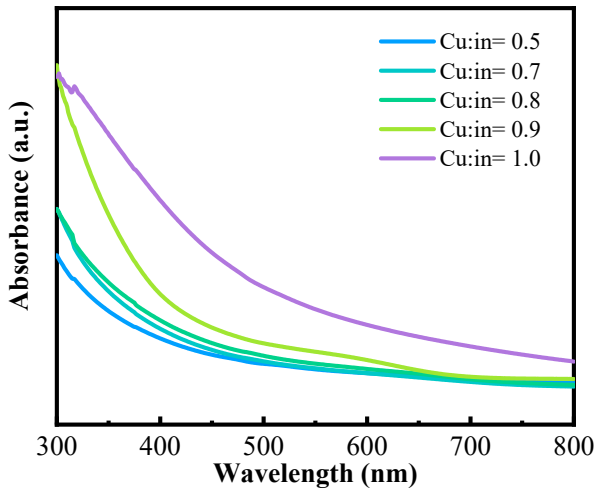

Fig. S3 The variation of the absorption spectrum of Zn: $CuInSe_2$/ZnS QDs with increasing the ratio of Cu.

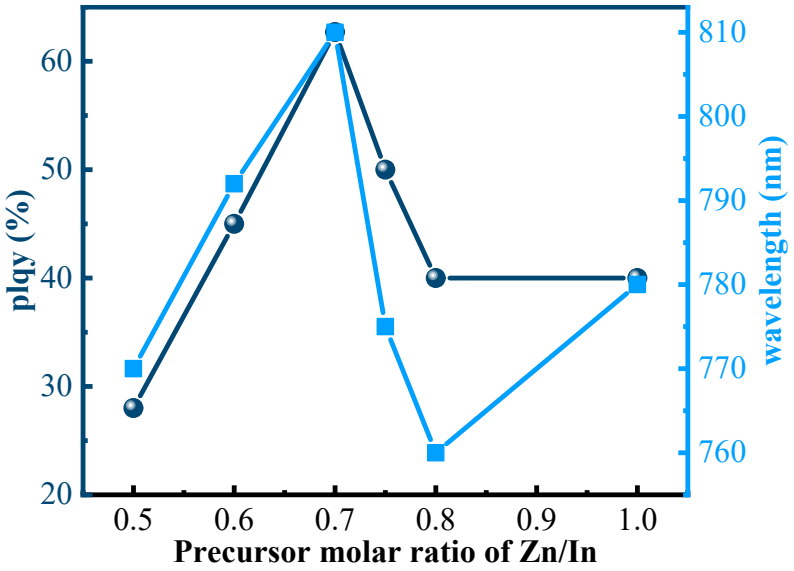

Fig. S4 The variations of PL peak wavelength and PLQY of Zn: $CuInSe_2$/ZnS QDs synthesized under different Zn/In molar ratios.

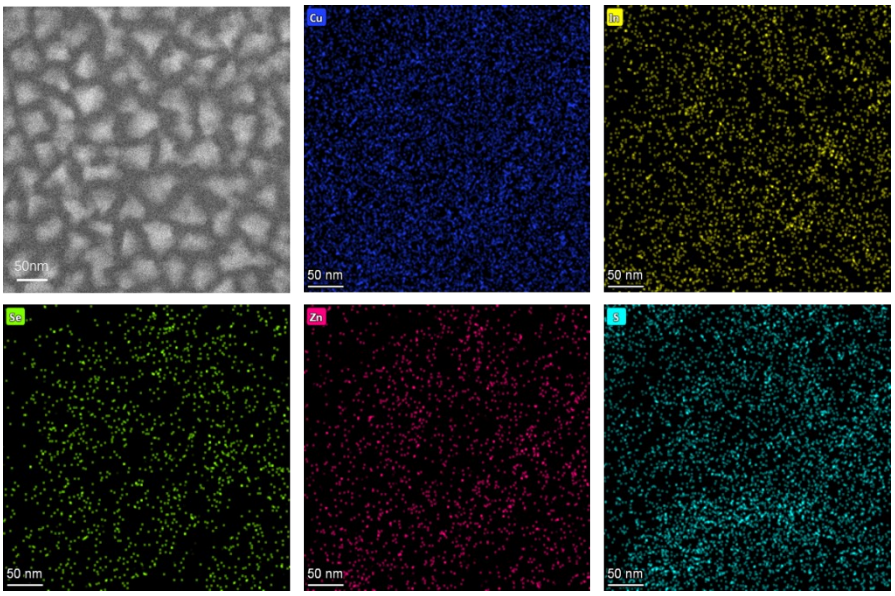

Fig. S5 Energy dispersive spectroscopy (EDS) image of Zn: $CuInSe_2$/ZnS revealing a uniform distribution of all constituent elements (Cu, In, Se, Zn, and S) in the Zn: $CuInSe_2$/ZnS QDs lattice.

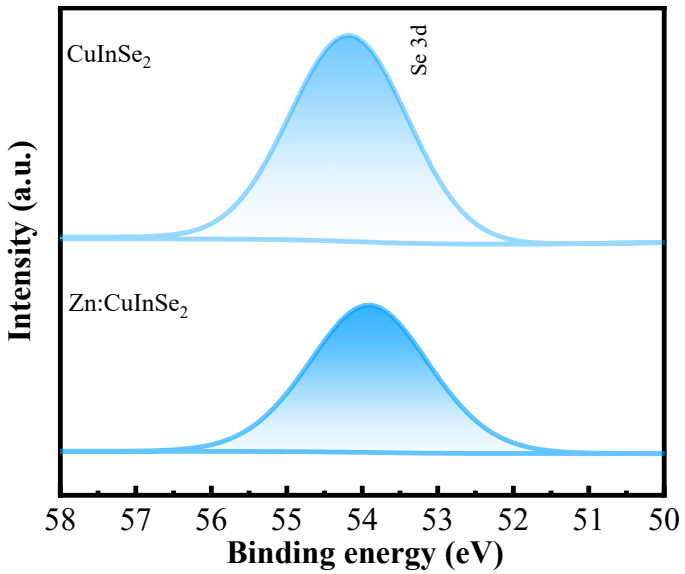

Fig. S6 High-resolution scans of the Se-3d XPS spectra.

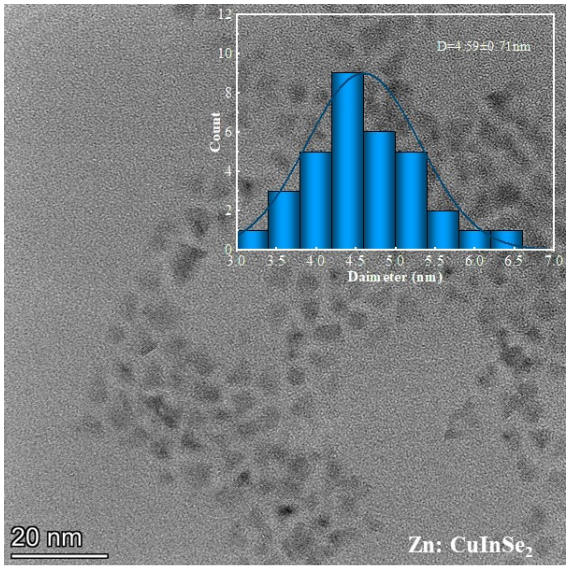

Fig. S7 Transmission electron microscopy (TEM) images and size distribution of Zn: $CuInSe_2$ QDs. It can be seen that all of the samples are very mono-dispersed without any aggregates and the average particle size is 4.59± 0.71 nm.

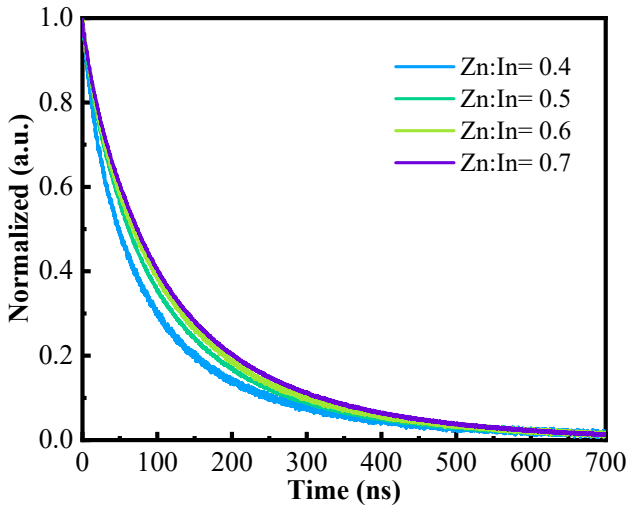

Fig. S8 The variation of the transient spectra of Zn: $CuInSe_2$/ZnS QDs with increasing the ratio of Zn.

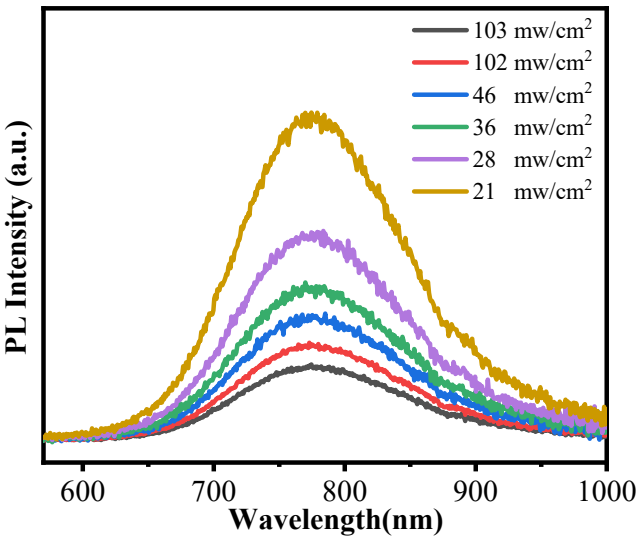

Fig. S9 Variation of PL spectra under different laser power levels.

Table S1. Comparison of the quantum dots synthesized in this work with different near-infrared material systems.

Year	Materials	Wavelength	PLQY	Application field	ref.
2024	$AgInS_2$	680 nm	24%	Biomedical Optical Imaging	32
2023	Zn: $CuInSe_2$/ZnS	780 nm	21%	Up-conversion Optics	33
2020	$CuInSe_2$/$CuInS_2$	950 nm	8%	Basic Materials Research	34
2022	$Cs_2Na_{1-x}Ag_xBi_{1-y}Al_yCl_6$ perovskite	715 nm	48.6%	Basic Materials Research	35
2024	InP	740 nm	52%	Basic Materials Research	36
2020	$Ag(InGa)Se_2$	800 nm	38%	Biomedical Optical Imaging	37
2024	$CuInSe_2$ /ZnS	878 nm	61%	Luminescent solar concentrator	38
2024	$CuInS_2$/ZnS	780 nm	70%	Luminescent solar concentrator	39
2020	$CuInSe_2$ ZnS	920-1224 nm	21.8%	Biomedical Optical Imaging	40
2024	**Zn: $CuInSe_2$/ZnS**	**810 nm**	**62.7%**	**NIR Wireless Communication**	**our work**

Table S2. Demonstrates the significant competitive advantage of the modulation bandwidth measured in this study within the near-infrared range.

Year	Application field	Modulation bandwidth	ref.
2020	NIR OLED	390 kHz	4
2023	High-speed OPD	4 MHz	61
2023	Photodetector	7.9 kHz	62
2021	white light-emitting diodes	1.5 MHz	63
2024	**NIR Wireless Communication**	**3.23 MHz**	**our work**